

Critical parameter estimates for earthquake forecast using PI migration

Yi-Hsuan Wu · John B. Rundle · Chien-chih Chen

Received: 25 August 2014 / Accepted: 6 December 2014 / Published online: 14 December 2014
© Springer Science+Business Media Dordrecht 2014

Abstract Parameters usually play a key role in statistical forecasting models and should be carefully determined because the physics of the system links to the statistical model through the parameters. To investigate the relations between parameters and pattern informatics (PI) migration, we developed a series of retrospective analyses. The results show that two parameters (i.e., cut magnitude and change interval) are essential factors of calculating PI migration. The cut magnitude is a lower cutoff magnitude applied to the catalog at the start of the analysis, and the result of the analysis shows that the PI migration hot spots are mostly distributed around the earthquakes with magnitude larger than target magnitude when the cut magnitude is 3.2–3.4 in most study regions. The change interval is a time span prior to the large event that we assumed to be the duration of the preparation process. In the retrospective analysis, the ability of PI migration hot spot to hit the target earthquake varies with change interval and the change interval that make PI migration hot spot to hit most target earthquakes varies with the study region. By using a retrospective analysis, we determined the optimal parameters for each study region, generating PI migration maps to show potential locations.

Keywords Pattern informatics · Relative intensity · Seismicity migration · Critical parameter

Y.-H. Wu · J. B. Rundle
Department of Geology, University of California, Davis, CA 95616, USA

Y.-H. Wu (✉) · C. Chen
Department of Earth Sciences, Graduate Institute of Geophysics, National Central University,
No. 300, Jhongda Rd., Jhongli City, Taoyuan County 32001, Taiwan, ROC
e-mail: maomaowyh@gmail.com; yhwu@ncu.edu.tw

J. B. Rundle
Department of Physics, University of California, Davis, CA 95616, USA

1 Introduction

The real dynamics of a complex system is unknown but it can be mapped by the use of pattern dynamics. In a complex system, the real underlying dynamics controls the physics of the system and produces the observable state variables. For example, we are unable to show the real dynamics of an earthquake system because of its nonlinearity and complexity, but we can observe some of the state variable events (i.e., seismicity) produced by this system. Observing seismicity patterns both in time and space enables constructing approximate dynamics and pattern dynamics that reflect the physics of the system. Pattern dynamics makes analyzing the dynamics of spatiotemporal patterns of seismicity an alternative approach to understand the real dynamics (Mori and Kuramoto 1997; Rundle et al. 2000a, b; Tiampo et al. 2002a, b).

The pattern informatics (PI) method is an example of a phase dynamical measure (Mori and Kuramoto 1997; Rundle et al. 2000a, b, 2003; Tiampo et al. 2002a, b; Chen et al. 2005, 2006) that is implemented for forecasting earthquakes by searching for seismicity rate deviations from average seismicity rates, including both seismic activation and quiescence (Wyss and Habermann 1988; Bowman et al. 1998; Jaume and Sykes 1999; Zoller et al. 2002; Chen et al. 2005; Nanjo et al. 2006; Huang 2008; Huang and Ding 2012). The activation and quiescence imply that the interaction between the faults may evolve into nucleation, reaching the driven threshold (Gomberg et al. 1998; Sornette 2002; Kawamura et al. 2012). To observe oriented fault growth, PI migration was proposed as a method to investigate the migration of anomalous seismicity, based on the PI method (Wu et al. 2008c, d, 2011).

Because of the interactions between faults, PI migration is sensitive to temporal, spatial, and seismic parameters (Wu et al. 2012). When testing the PI migration, obtaining the optimal results or parameter values associated with the tectonic setting requires capturing the nontrivial relation between the model parameters and statistical model. In other words, it must be determined how a forward statistical model, such as PI migration, varies in response to model parameter changes. Similarly, an inverse statistical model that maps the results of the statistical model to the model parameters indicates the specific values of the model parameters, based on desired statistical model values. This latter procedure can be considered to be a type of data assimilation.

To capture the relationship between model parameters and the statistical model, we analyzed the PI migration using varying model parameters. We assumed that the PI migration statistical model could forecast earthquakes exhibiting magnitudes larger than the target magnitude in the future year. The spatial parameters of PI migration, spatial region, and depth, which are associated with the earthquake system and its tectonic setting, can be selected according to the seismicity distribution. Other essential parameters that PI migration replies on, such as temporal parameters and the cut magnitude, cannot be selected using seismicity distribution and must be estimated based on PI migration analysis.

Our results showed strong correlations of cut magnitude and change interval with PI migration. The cut magnitude is a lower cutoff magnitude applied to the catalog at the start of the analysis, and the result of the analysis shows that the PI migration hot spots are mostly distributed around the earthquakes with magnitude larger than target magnitude when the cut magnitude is 3.2–3.4 in most study regions. The change interval is a time span prior to the large event that we assumed to be the duration of the preparation process. In the retrospective analysis, the ability of PI migration hot spot to hit the target earthquake varies with change interval and the change interval that make PI migration hot spot to hit most

target earthquakes varies with the study region. The relation between the change interval and study region indicates that PI migration is dominated by the stress interaction. We also show the PI migration with the optimal parameters obtained from the retrospective analysis.

2 PI migration calculation

We take the average number of earthquakes with magnitude larger than the cut magnitude M_c as a state variable in pattern dynamics (Rundle et al. 2000a; Tiampo et al. 2002a, b; Chen et al. 2005; Holliday et al. 2007; Wu et al. 2008c, d, 2011). The average number of earthquakes of $M \geq M_c$ in the grid box centered at x_i and its Moore neighbor boxes during the time interval t_b to t is defined as the seismic intensity $I(x_i, t_b, t)$, as

$$I(x_i, t_b, t) \equiv \frac{1}{(t - t_b)} \int_{t_b}^t n(x_i, t) dt \tag{1}$$

where $n(x_i, t)$ is the number of events at location x_i and time t and t_b is the sampling time that shifts from the start of dataset, t_0 , to the beginning of change interval, t_1 . The change of seismic intensity within the change interval, t_1 to t_2 , is defined as

$$\Delta I(x_i, t_b) = I(x_i, t_b, t_1) - I(x_i, t_b, t_2). \tag{2}$$

Consequently, the change of seismicity intensity is normalized in time and space to accent the anomalous seismic intensity as

$$\tilde{I}(x_i, t_b) = \frac{\Delta I_{x_i}(t_b) - \overline{\Delta I}_{x_i}(t_b)}{\sigma_{x_i}(t_b)} \tag{3.1}$$

and

$$\hat{I}(x_i, t_b) = \frac{\tilde{I}_{t_b}(x_i) - \bar{\tilde{I}}_{t_b}(x_i)}{\bar{\sigma}_{t_b}(x_i)} \tag{3.2}$$

where $\overline{\Delta I}_{x_i}(t_b)$ and $\sigma_{x_i}(t_b)$ in Eq. (3.1) are the mean and standard deviation of the seismic intensity change taken at each x_i ; $\bar{\tilde{I}}_{t_b}(x_i)$ and $\bar{\sigma}_{t_b}(x_i)$ in Eq. (3.2) are the mean and standard deviation of temporally normalized seismic intensity change at each t_b . Positive $\hat{I}(x_i, t_b)$ indicates intense seismic activity, and negative $\hat{I}(x_i, t_b)$ indicates weak seismic activity. To involve all seismic anomalies and reduce the fluctuation caused by random noise, the absolute $\hat{I}(x_i, t_b)$ was averaged to all t_b , denoted as $|\overline{\hat{I}(x_i, t_b)}|$. The probability of an event occurring at x_i is defined as

$$P(x_i) = \left| \overline{\hat{I}(x_i, t_b)} \right|^2. \tag{4}$$

The relative probability at x_i compared with an entire region is defined as

$$\Delta P(x_i) = \left| \overline{\hat{I}(x_i, t_b)} \right|^2 - \mu_p. \tag{5}$$

where μ_p is the mean of $P(x_i)$ over all x_i . The location with high relative probability, which is higher than the given threshold, is shown as the hot spot on the PI map.

To quantify the migration of the PI hotspot, we defined the error distance $\varepsilon(t)$ as the distance between the center of the grid box and the nearest hot spot at time t during the change interval. Because the threshold given in the PI map controls the number of PI hot spots and thus the error distance, we integrated the error distance to eliminate the threshold constraint, denoted as $\varepsilon_{\text{area}}(t)$. Figure 2 of Wu et al. (2008d) illustrates the calculation of $\varepsilon_{\text{area}}(t)$. For each grid box, the integrated error distance is a function of time. A slope that shows the movement of the PI hot spot for each grid box can be obtained by fitting the $\varepsilon_{\text{area}}(t)$ over a time period. A grid box exhibiting a negative slope identifies the location toward where the PI hot spots migrate. The shifting time t used in PI migration calculation is a sampled time; its interval $[t_{1\text{st}}, t_{1\text{en}}]$ is defined as migration time. Start of migration time $t_{1\text{st}}$ typically is the onset of the change interval t_1 , and end of migration time $t_{1\text{en}}$ is a time in the middle of the change interval $[t_1, t_2]$. A whole flowchart of the procedure for obtaining PI maps and the schematic diagram for obtaining PI migration map can be seen in Fig. 3 of Kawamura et al. (2013).

3 Data, parameter, and hit ratio

The regions of interest in this study are Taiwan, Japan, and California because numerous earthquakes occur in these regions and sophisticated earthquake catalogs are available. We selected the seismicity data for Taiwan, Japan, and California from the Central Weather Bureau (CWB), the Japan Meteorological Agency (JMA), and the Advanced National Seismic System (ANSS) earthquake catalogs, respectively. Only the earthquakes with magnitude larger than cut magnitude M_c are involved in the PI migration calculation because those smaller than cut magnitude may not be able to indicate the precursory seismicity. Considering the completeness of the catalog, the starting time of the seismicity data (i.e., t_0) used for Taiwan is 1990, 1985 for Japan, and 1980 for California.

The study regions were divided into subregions and assigned a depth according to the tectonic setting. We did not include seismicity data from beneath the given depth in the calculation because of the possible association with other earthquake systems that might differ from earthquake systems in the upper crust (Tsai 1986; Kagan 1992). We divided the Taiwan region into western Taiwan, eastern Taiwan, and northeastern Taiwan (Wu et al. 2008a). The Japan region was divided into southwestern Japan, northeastern Japan, and the Kanto region (Seno et al. 1993). The California region was divided into northern California and southern California. We chose seismicity data within a depth of 0–20 km for western Taiwan, 0–30 km for eastern Taiwan, and 0–50 km for northeastern Taiwan based on seismicity distribution and tectonics (Kim et al. 2005; Wu et al. 2008a, b). We assigned cut depths of 60 km to southwestern Japan, 150 km to northeastern Japan, and 30 km to the Kanto region (Yoshi 1979; Peacock and Wang 1999; Sato et al. 2005; Nakajima and Hasegawa 2010; Uchida et al. 2010). Regarding both northern and southern California, the cut depth was 15 km (Mori and Abercrombie 1997).

To demonstrate which parameters cause the most substantial system changes and reflect events in the future year, we quantified the correlations between the parameters, change interval $[t_1, t_2]$, cut magnitude M_c , and future events. The change interval varied from 2 to 5.5 years (with a step of interval 0.5 years), and the cut magnitude ranged from 3.0 to 4.0 (with a step of interval 0.2). We calculated the PI migration by using seismicity data for various sets of change intervals and cut magnitudes in the examining period, subsequently examining whether events with magnitudes larger than the target magnitude occurred on the hot spots determined using the PI migration. The examining period included the time

from the onset of the seismicity data to the beginning of the change interval, t_0 to t_1 , and the change interval, t_1 to t_2 . We assigned the migration time parameter as 1.5, 2.0, 2.5, and 3.0 years at the onset of the change interval. The remaining change interval times, excluding the migration time, were 0.5, 1.0, 1.5, 2.0, and 2.5 years. The test period was one year following the end of change interval t_2 . We sampled the test period from July 2004 to July 2010 in Taiwan and Japan and from 2005 to 2011 in California per half year. To quantify the correlation between parameter sets and future events, we defined a hit ratio, $N_{\text{hit}}/N_{\text{all}}$, where N_{all} is the number of hot spots obtained from the PI migration calculation and N_{hit} is the number of hot spots with future events that is larger than the target magnitude occurring in the same location. Considering that the empirical test would not be statistically reliable if too few events with magnitudes larger than the target magnitude occurred in the test period, we assigned target magnitudes of 5.0 for western Taiwan and California, and 5.5 for eastern Taiwan, northeastern Taiwan, and Japan.

4 Results

Figures 1, 2, and 3 show the diagrams of hit ratio of PI migration versus the change interval t_2-t_1 using different cut magnitude M_c for the study regions of Taiwan, Japan, and California. The open circle, solid circle, open triangle, and solid triangle means 1.5, 2.0, 2.5, and 3.0 years of migration time $t_{1\text{en}}-t_{1\text{st}}$, respectively. In most regions, we can obtain a relation between hit ratio and change interval (i.e., the hit ratio clearly increase or decrease with the change interval in a range) with a particular range of cut magnitude M_c .

Figure 1a–c shows the hit ratios of PI migration, using various parameter sets in the western Taiwan, the eastern Taiwan, and the northeastern Taiwan regions, respectively. A stable hit ratio trend is observed (i.e., the hit ratio varies based on the change interval t_2-t_1 when the cut magnitude is between 3.2 and 3.6 for the western Taiwan region; Fig. 1a), and a high value is yielded when the change interval t_2-t_1 is 3.0 years. However, the hit ratio is not dependent on the length of the migration time for $M_c = 3.2-3.6$ in western Taiwan. The overall value of hit ratio for eastern Taiwan (Fig. 1b) decreases from $M_c = 3.0$ to $M_c = 4.0$, and a high value is yielded when the change interval is 3.5 or 4.0 years. The hit ratio tends to decrease as the change interval increases in length when the change interval is longer than 3.5 years. No relation exists between the hit ratio and migration time in eastern Taiwan; the highest hit ratio at each given cut magnitude is obtained at varying migration time. Northeastern Taiwan also demonstrates a stable hit ratio trend (Fig. 1c), showing similar variations with the change interval at all cut magnitudes. A high hit ratio can be obtained when the cut magnitude is 3.4, the change interval is 5.0 years, and the migration time is 3.0 years.

Figure 2a–c shows the hit ratio results for the northeastern Japan, Kanto, and southwestern Japan regions. Figure 2a shows that the overall hit ratio for northeastern Japan decreases as the cut magnitude increases and the value drops when the change interval is larger than 4.0 years. There is not a clear relation between the hit ratio and migration time in northeastern Japan. A relatively high hit ratio can be obtained when the change interval is 3.5–4.0 years for all cut magnitudes. The hit ratio for the Kanto region (Fig. 2) is low when the change interval is smaller than 3.0 years for all cut magnitudes. The hit ratio increases when the change interval is 3.0 years, and the hit ratio gradually decreases for most cut magnitudes. The hit ratio dramatically increases at 3.0–3.4 of the cut magnitude when the migration time is 2 years. Figure 2c shows a clear relation between the hit ratio and change interval for all cut magnitudes in the southwestern Japan region; the hit ratio

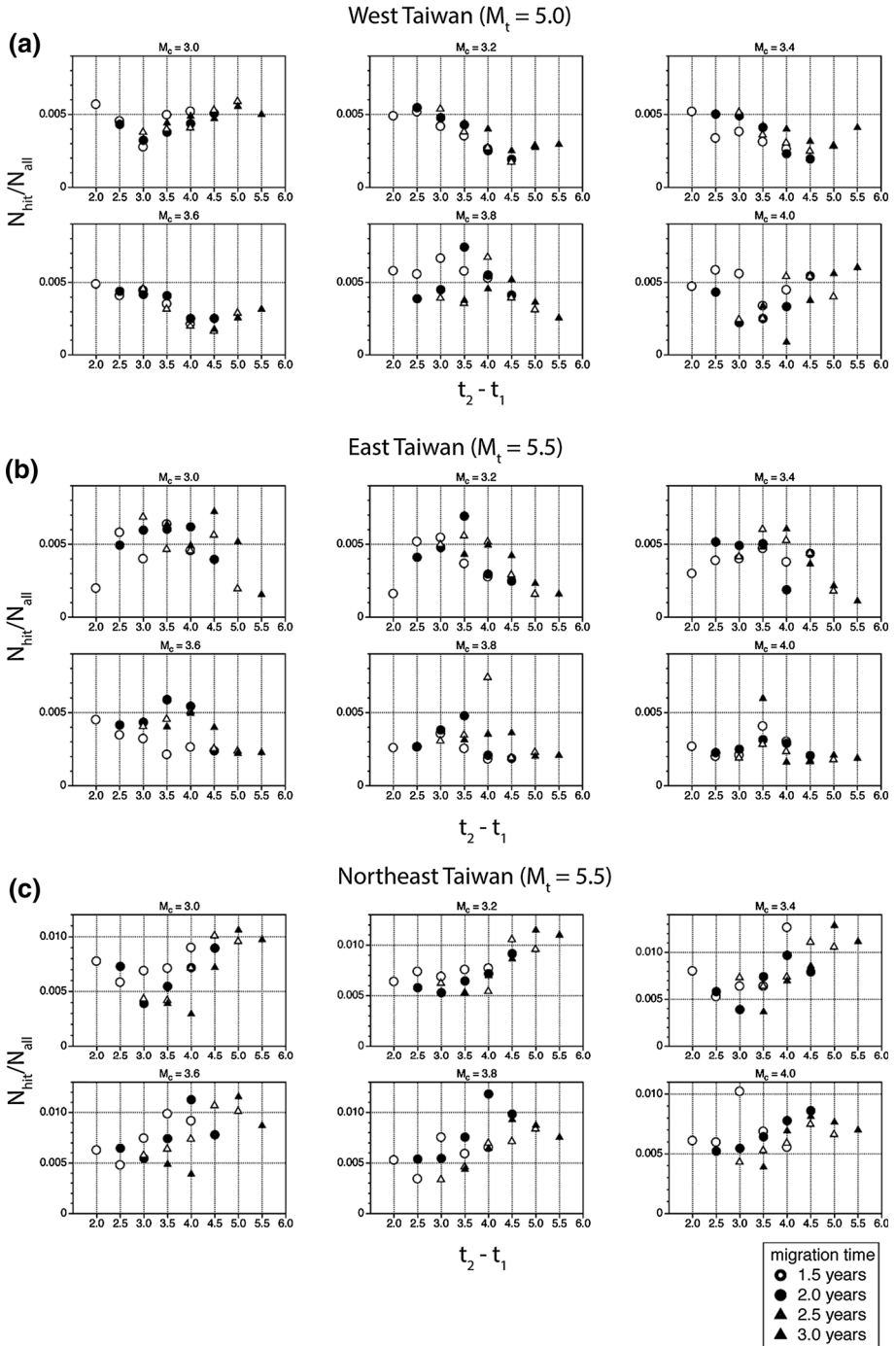


Fig. 1 Hit ratio N_{hit}/N_{all} versus the change interval t_2-t_1 at various migration times and cut magnitudes (from the upper left to the lower right) for **a** the western Taiwan, **b** eastern Taiwan, and **c** northeastern Taiwan regions

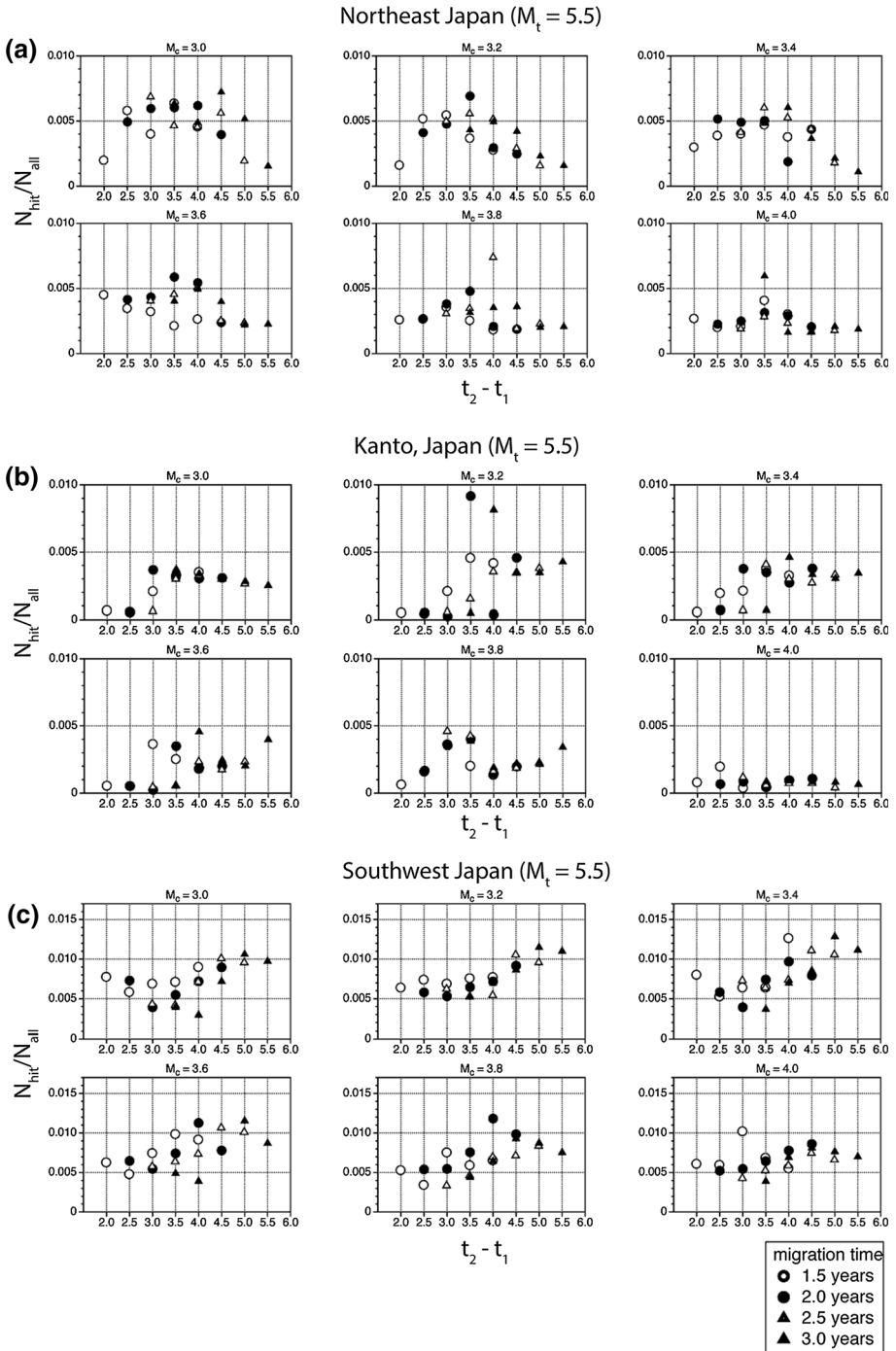


Fig. 2 Hit ratio N_{hit}/N_{all} versus the change interval t_2-t_1 at various migration times and cut magnitudes (from the upper left to the lower right) for **a** the northeastern Japan, **b** Kanto, and **c** southwestern Japan regions

decreases from a change interval of 2.0 years to 3.0 years, increases to its highest value from 3.0 years to 5.0 or 4.5 years, and decreases again. The overall hit ratio increases from $M_c = 3.0$ to $M_c = 3.4$ and decreases from $M_c = 3.6$ to $M_c = 4.0$. A highest hit ratio for a cut magnitude of 3.0–3.6 can be obtained at a change interval of 5.0 years and a migration time of 3.0 years.

Figure 3a, b shows the hit ratio results for the northern and southern California regions, respectively. It is difficult to determine the relations between the hit ratio, change interval, cut magnitude, and migration time in northern California (Fig. 3a). However, we can obtain a high hit ratio when the cut magnitude is 3.2, 3.6, or 3.8 and the change interval is 2.0–2.5 years. The southern California results (Fig. 3b) show a strong relation between the hit ratio and change interval, particularly when the cut magnitude is 3.2–3.6. The hit ratio dramatically increases when the change interval is larger than 4.0 years. The largest hit ratio can be obtained at a change interval of 5.5 years for most cut magnitudes.

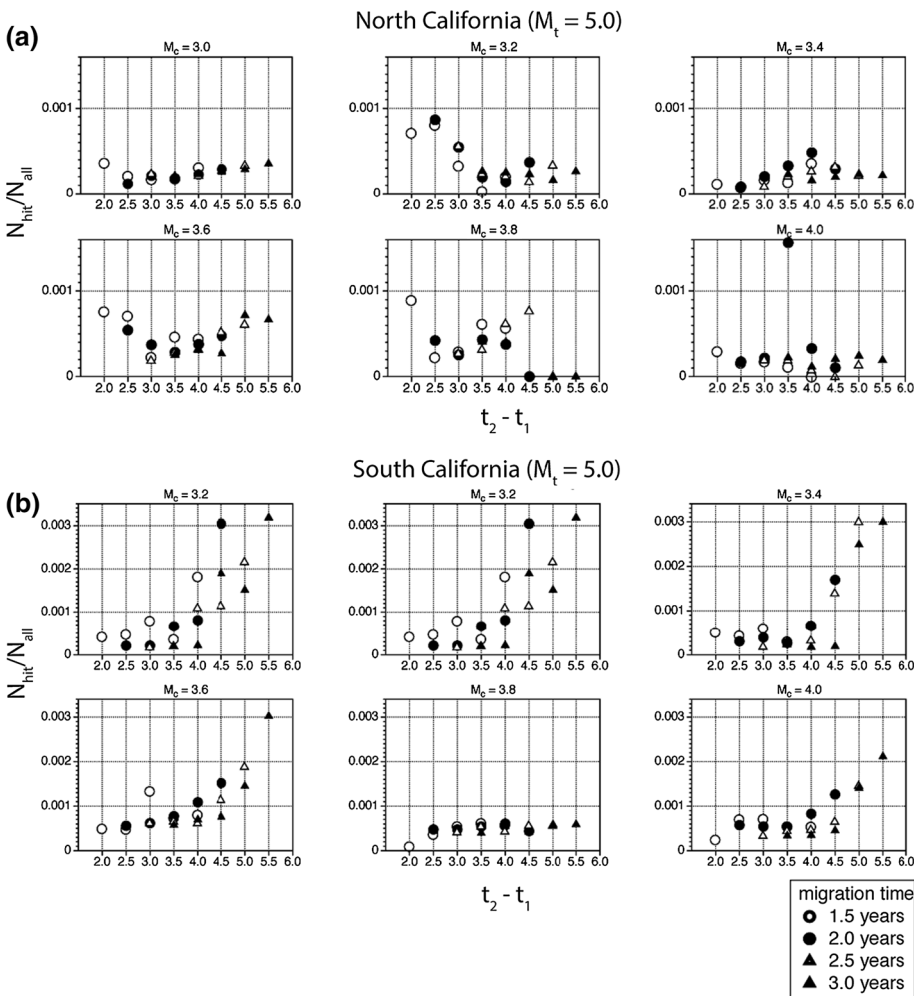


Fig. 3 Hit ratio N_{hit}/N_{all} versus the change interval t_2-t_1 at various migration times and cut magnitudes (from the upper left to the lower right) for **a** the northern and **b** southern California regions

5 Discussion and conclusion

Numerous statistical methods have been applied to forecast events in natural physical systems (Kagan and Jackson 2000; Huang et al. 2001; Huang 2004; Holliday et al. 2005; Chen et al. 2005, 2006; Chen and Wu 2006; Lee et al. 2011; Rundle et al. 2011; Wu et al. 2011). There are some attempts on optimal estimation of parameters in some statistical methods (Wu and Chen 2007; Huang and Ding 2012). However, a common difficulty in formulating a precise forecast is estimating the critical parameter values. To calculate the parameter values, we constructed a simple analysis to retrospectively investigate the relations between the parameters and PI migration. The results indicated the correlations between the PI migration, cut magnitude, and change interval.

The cut magnitude is a lower bounding magnitude that is provided to eliminate small earthquakes from analyses. Determining a cut magnitude removed most aftershocks and the incomplete catalog from the background and highlighted anomalous seismicity. In most study regions, a 3.2 or 3.4 cut magnitude caused the PI migration to hit most events. Fault nucleation and growth have been observed in the laboratory and in models (Liakopoulou-Morris et al. 1994; Reches and Lockner 1994; Ellsworth and Beroza 1995; Clifton and Schlische 2001). Because seismicity migrates toward the direction in which the fault grows, PI migration might be caused by fault nucleation, and the faults that yield $M = 3.2\text{--}3.4$ earthquakes could be natural nucleation zones.

The change interval is the phase transition period before the critical point, or the duration of preparation process. Anomalous seismicity during the preparation process, such as activation and quiescence, causes a state variable shift in pattern dynamics and a high PI probability. Calculating the precise PI migration requires tracing PI hot spots exhibiting high probability. A change interval that includes the greatest anomalous seismicity and the least background and noise facilitates calculating PI migration. In most of the study regions, the number of PI migration hot spots hitting the events varied based on the change interval and a dominant change interval that causes the PI migration hot spots to hit most events exists within a specific cut magnitude range. The results show a relation between the hit ratio and the change interval in all study regions. In contrast to the change interval, another time parameter, migration time, which is used to trace the PI hot spots, does not show a relation with the hit ratio.

Wu et al. (2012) showed that seismicity selection influences migration patterns because of regional tectonics. Seismicity selection should consider the area and depth to maintain a simple seismotectonic setting in the study region. We showed that the seismotectonic setting might influence the parameters. We found that the hit ratios indicated similar dominant parameter patterns in the northeastern Taiwan and southwestern Japan regions. A higher hit ratio is found in the northeastern Taiwan and the southwestern Japan regions compared with other study regions. In addition, similar parameters contributed to high hit ratios in these regions: a cut magnitude of 3.4 and change interval of 5 years. These similar results may be a consequence of the Nankai Trough system, to which the northeastern Taiwan and the southwestern Japan regions belong.

We applied the parameter values that yielded high ratios in the study regions to calculate PI migration. Table 1 lists the implemented parameter values and cut depths. The cut depth denoted as D_c in Table 1 is the lower bound of depth of the study region, determined based on the seismicity distribution and tectonic settings (Yoshi 1979; Mori and Abercrombie 1997; Peacock and Wang 1999; Kim et al. 2005; Sato et al. 2005; Wu et al. 2008a, b; Nakajima and Hasegawa 2010; Uchida et al. 2010). The M_c and M_t denote the cut magnitude and target magnitude, respectively. The cut magnitude is the lower

Table 1 Optimal parameter values for PI migration obtained from retrospective analysis

	Taiwan			Japan			California	
	West	East	Northeast	Southwest	Kanto	Northeast	North	South
D_c (km)	20	30	50	60	30	150	15	15
M_c	3.2	3.2	3.4	3.4	3.2	3.2	3.2	3.2
M_t	5.0	5.5	5.5	5.5	5.5	5.5	5.0	5.0
t_2-t_1 (years)	3.0	3.5	5.0	5.0	3.5	3.5	2.5	5.5
$t_{1en}-t_{1st}$ (years)	2.5	2.0	3.0	3.0	2.0	2.0	2.0	3.0

Fig. 4 PI migration map for the Taiwan region. The *upper panel* is valid for the time from April 2014 to April 2015, and the *bottom panel* is valid for the time from July 2014 to July 2015. The *circles* show the earthquakes with magnitude larger than M_t listed in Table 1 that occurred before 2014/11/30. The *gray dash line* distinguishes the western, eastern, and northeastern Taiwan regions. The *color bar* shows the intensity (slope) of the PI migration; the *warm colors* represent high intensity (negative slope)

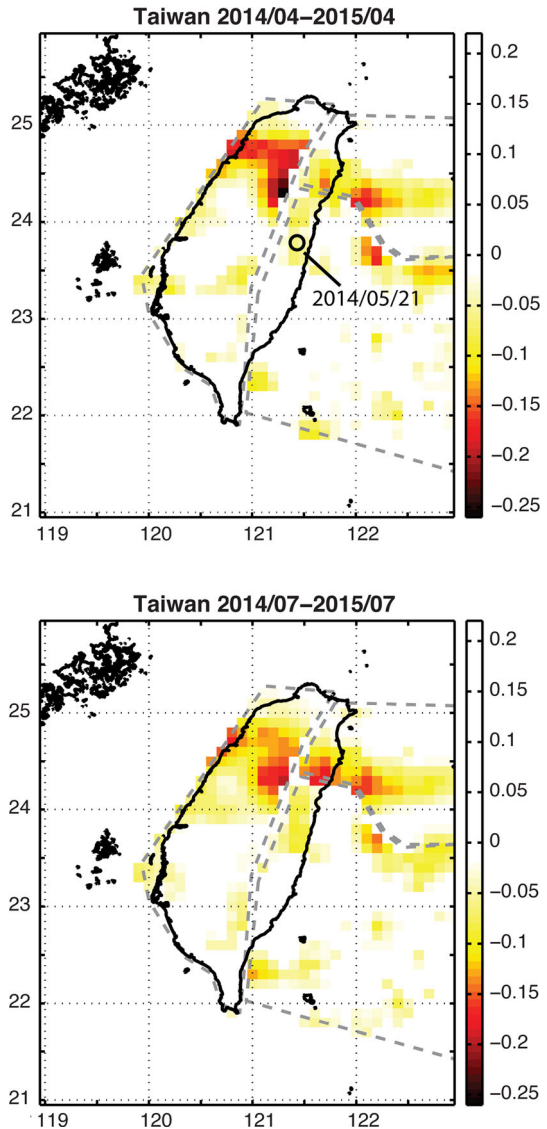
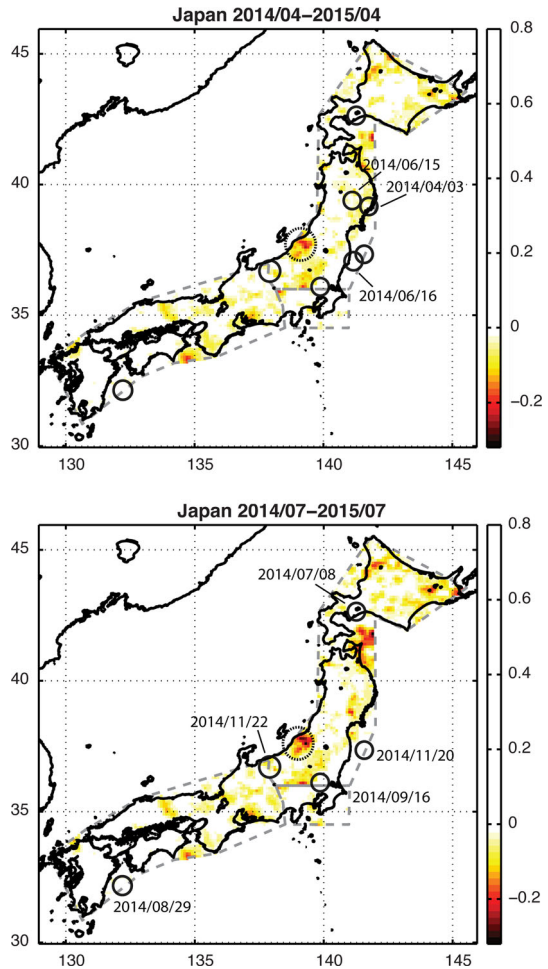


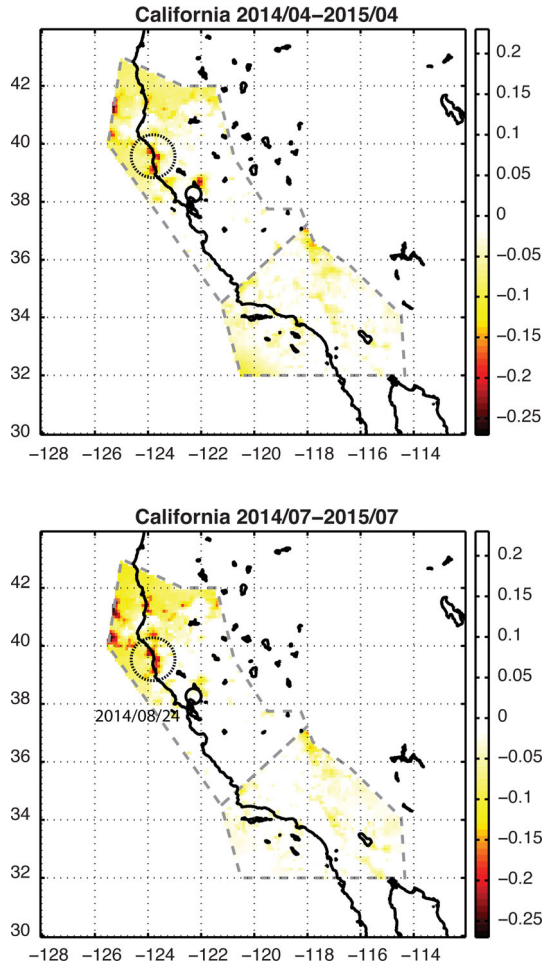
Fig. 5 PI migration map for the Japan region. The *upper panel* is valid for the time from April 2014 to April 2015, and the *bottom panel* is valid for the time from July 2014 to July 2015. The *circles* show the earthquakes with magnitude larger than M_t listed in Table 1 that occurred before 2014/11/30. The *gray dash line* distinguishes the northeastern Japan, Kanto, and southwestern Japan regions. The *color bar* shows the intensity (slope) of the PI migration; the *warm colors* represent high intensity (negative slope)



bounding magnitude for calculating PI migration, and the target magnitude is the magnitude of events. In certain regions that exhibited low seismic activity levels, we estimated only the parameters for $M_t = 5.0$. The change interval and migration time set in the PI migration calculation were $t_2 - t_1$ and $t_{1en} - t_{1st}$, respectively (Table 1).

To facilitate efficient forecasting, we formulated the PI migration at the onset of each quarter. Using the parameter setting shown in Table 1, we calculated the PI migration for the Taiwan, Japan, and California regions shown in Figs. 4, 5, and 6, respectively. In Figs. 4, 5, and 6, the top panel is the PI migration map with the end of the change interval $t_2 = 2014/04/01$ and the bottom panel is for $t_2 = 2014/07/01$. The dashed gray line shows the boundary of each study region. The circles in Figs. 4, 5, and 6 show the earthquakes with magnitude larger than M_t listed in Table 1 that occur during t_2 to 2014/11/30. It can be observed that some strong hot spots occur in the western Taiwan (Fig. 4) due to the earthquake with magnitude larger than M_t occurred at 2014/05/21. Because of its aftershocks, the strong hot spots in the western Taiwan become weaker but not disappear when the PI migration map is for 2014/07/01. In Japan, some hot spots that occur around the

Fig. 6 PI migration map for the California region. The *upper panel* is valid for the time from April 2014 to April 2015, and the *bottom panel* is valid for the time from July 2014 to July 2015. The *circles* show the earthquakes with magnitude larger than M_t listed in Table 1 that occurred before 2014/11/30. The *gray dash line* distinguishes the northern and southern California regions. The *color bar* shows the intensity (slope) of the PI migration; the warm colors represent high intensity (negative slope)



earthquakes with magnitude larger than M_t that occurred after July in the top panel of Fig. 5 become intense in the bottom panel of Fig. 5. The result in Japan suggests us to pay attention to the location with hot spots getting intense such as the place denoted by dashed circle in Fig. 5. In California (Fig. 6), most intense hot spots are located in northern California in the top panel; one group is close to the earthquake with magnitude larger than M_t occurred at 2014/08/24, and another group is at where we denoted by dashed circle. The hot spots in the dashed circle should be paid attention to because they become more intense when time moves on.

We determined the relations between parameters and PI migration, considering the hit ratio as a reference index to facilitate comparing the effects of various parameter sets. Because the hit ratio is a ratio between the number of hot spots that hit events and the total number of hot spots, a high hit ratio may be caused by low noise levels or a small migration range. Because of the tectonic setting, the seismicity varies from region to region and the PI migration yields various migration ranges; thus, the level of hit ratio may also reflect the tectonic properties of the region.

The relation between the PI migration range and the tectonics is a concern. The PI migration range may be associated with fault types and event magnitudes, which are related to the stress accumulation caused by tectonics. Clarifying the relation between the PI migration range and tectonics may enhance forecasting accuracy. However, examining this relation requires precisely quantifying the PI migration range and lies outside the scope of this study.

We examined the relations between parameters and PI migration by using retrospective analysis. Our results show that two parameters (i.e., cut magnitude and change interval) are essential for calculating PI migration. The result of the analysis shows that the PI migration hot spot is able to hit most target events when the cut magnitude is 3.2–3.4 in most study regions. The change interval varies among regions, indicating the duration required for the preparation process is different. By using retrospective analysis, we obtained the optimal parameters for the study regions and demonstrated potential PI migration locations. Our results suggest that calculating PI migration in regular facilitates detecting earthquakes.

Acknowledgments The authors would like to express their gratitude to the Central Weather Bureau (CWB), National Research Institute for Earth Science and Disaster Prevention (NIED), and Advanced National Seismic System (ANSS) for providing their quality earthquake catalogs. The research by JBR was supported by a grant to U.C. Davis (grant NASA NNX12AM22G). The work of YHW and CCC was supported by the National Science Council (ROC) and the Department of Earth Sciences, NCU (ROC). YHW and CCC would like to acknowledge the support of the Ministry of Science and Technology (ROC).

References

- Bowman DD, Ouillon G, Sammis CG, Sornette A, Sornette D (1998) An observational test of the critical earthquake concept. *J Geophys Res* 103:24359–24372
- Chen CC, Wu YH (2006) An improved region-time-length algorithm applied to the 1999 Chi-Chi, Taiwan earthquake. *Geophys J Int* 166:1144–1147
- Chen CC, Rundle JB, Holliday JR, Nanjo KZ, Turcotte DL, Li SC, Tiampo KF (2005) The 1999 Chi-Chi, Taiwan, earthquake as a typical example of seismic activation and quiescence. *Geophys Res Lett* 32:L22315. doi:10.1029/2005GL023991
- Chen CC, Rundle JB, Li HC, Holliday JR, Nanjo KZ, Turcotte DL, Tiampo KF (2006) From tornadoes to earthquakes: forecast verification for binary events applied to the 1999 Chi-Chi, Taiwan, Earthquake. *Terr Atmos Ocean Sci* 17:503–516
- Clifton AE, Schlische RW (2001) Nucleation, growth, and linkage of faults in oblique rift zones: results from experimental clay models and implications for maximum fault size. *Geology* 29:455–458
- Ellsworth WL, Beroza GC (1995) Seismic evidence for an earthquake nucleation phase. *Science* 268:851–855
- Gomberg J, Beeler NM, Blanpied ML, Bodin P (1998) Earthquake triggering by transient and static deformations. *J Geophys Res* 103:24411–24426
- Holliday JR, Nanjo KZ, Tiampo KF, Rundle JB, Turcotte DL (2005) Earthquake forecasting and its verification. *Nonlin Process Geophys* 12:965–977. doi:10.5194/npg-12-965-2005
- Holliday JR, Chen CC, Tiampo KF, Rundle JB, Turcotte DL, Donnellan A (2007) A RELM earthquake forecast based on pattern informatics. *Seismol Res Lett* 78:87–93
- Huang QH (2004) Seismicity pattern change prior to large earthquakes—an approach of the RTL algorithm. *Terr Atmos Ocean Sci* 15:469–491
- Huang QH (2008) Seismicity changes prior to the M_S 8.0 Wenchuan earthquake in Sichuan, China. *Geophys Res Lett* 35:L23308. doi:10.1029/2008GL036270
- Huang QH, Ding X (2012) Spatiotemporal variations of seismic quiescence prior to the 2011 M 9.0 Tohoku earthquake revealed by an improved region–time–length algorithm. *Bull Seismol Soc Am* 102:1878–1883
- Huang QH, Sobolev G, Nagao T (2001) Characteristics of the seismic quiescence and activation patterns before the $M = 7.2$ Kobe earthquake, January 17, 1995. *Tectonophysics* 337:99–116
- Jaume SC, Sykes LR (1999) Evolving towards a critical point: a review of accelerating seismic moment/energy release prior to large and great earthquakes. *Pure appl Geophys* 155:279–306

- Kagan YY (1992) On the geometry of an earthquake fault system. *Phys Earth Planet Int* 71:15–35
- Kagan YY, Jackson DD (2000) Probabilistic forecasting of earthquakes. *Geophys J Int* 143:438–453
- Kawamura H, Hatano T, Kato N, Biswas S, Chakrabarti BK (2012) Statistical physics of fracture, friction and earthquake. *Rev Mod Phys* 84:839–884
- Kawamura M, Wu YH, Kudo T, Chen CC (2013) Precursory migration of anomalous seismic activity revealed by the pattern informatics method: a case study of the 2011 Tohoku earthquake, Japan. *Bull Seismol Soc Am* 103:1171–1180
- Kim KH, Chiu JM, Pujol J, Chen KC, Huang BS, Yeh YH, Shen P (2005) Three-dimensional V_p and V_s structural models associated with the active subduction and collision tectonics in the Taiwan region. *Geophys J Int* 162:204–220
- Lee YT, Turcotte DL, Holliday JR, Sachs MK, Rundle JB, Chen CC, Tiampo KF (2011) Results of the regional earthquake likelihood models (RELM) test of earthquake forecasts in California. *Proc Natl Acad Sci USA* 108:16533–16538
- Liakopoulou-Morris F, Main IG, Crawford BR, Smart GD (1994) Microseismic properties of a homogeneous sandstone during fault nucleation and frictional sliding. *Geophys J Int* 119:219–230
- Mori J, Abercrombie RE (1997) Depth dependence of earthquake frequency–magnitude distributions in California: implications for rupture initiation. *J Geophys Res* 102:15081–15090
- Mori H, Kuramoto Y (1997) Dissipative structures and chaos. Springer, New York
- Nakajima J, Hasegawa A (2010) Cause of $M \sim 7$ intraslab earthquakes beneath the Tokyo metropolitan area, Japan: possible evidence for a vertical tear at the easternmost portion of the Philippine Sea slab. *J Geophys Res* 115:B04301
- Nanjo KZ, Holliday JR, Chen CC, Rundle JB, Turcotte DL (2006) Application of a modified pattern informatics method to forecasting the locations of future large earthquakes in the central Japan. *Tectonophysics* 424:351–366
- Peacock SM, Wang K (1999) Seismic consequences of warm versus cool subduction metamorphism: examples from southwest and northeast Japan. *Science* 286:937–939
- Reches Z, Lockner DA (1994) Nucleation and growth of faults in brittle rocks. *J Geophys Res* 99(B9):18159–18173. doi:[10.1029/94JB00115](https://doi.org/10.1029/94JB00115)
- Rundle JB, Klein W, Tiampo KF, Gross S (2000a) Linear pattern dynamics in nonlinear threshold systems. *Phys Rev E* 61:2418–2432
- Rundle JB, Klein W, Gross S, Tiampo KF (2000b) Dynamics of seismicity patterns in systems of earthquake faults. In: Rundle JB, Turcotte DL, Klein W (eds) *Geocomplexity and the physics of earthquakes*. American Geophysical Union, Washington, DC, pp 127–146
- Rundle JB, Turcotte DL, Shcherbakov R, Klein W, Sammis C (2003) Statistical physics approach to understanding the multiscale dynamics of earthquake fault systems. *Rev Geophys* 41(4):1019. doi:[10.1029/2003RG000135](https://doi.org/10.1029/2003RG000135)
- Rundle JB, Holliday JR, Yoder M, Sachs MK, Donnellan A, Turcotte DL, Tiampo KF, Klein W, Kellogg LH (2011) Earthquake precursors: activation or quiescence? *Geophys J Int* 187:225–236
- Sato H, Hirata N, Koketsu K, Okaya D, Abe S, Kobayashi R, Matsubara M, Iwasaki T, Ikawa T, Kawanaka T, Ito T, Kasahara K, Harder S (2005) Earthquake source fault beneath Tokyo. *Science* 309:462–464
- Seno T, Stein S, Gripp AE (1993) A model for the motion of the Philippine Sea plate consistent with NUVEL-1 and geological data. *J Geophys Res* 89:17941–17948
- Sornette D (2002) Predictability of catastrophic events: material rupture, earthquakes, turbulence, financial crashes, and human birth. *Proc Natl Acad Sci USA* 99:2522–2529
- Tiampo KF, Rundle JB, McGinnis S, Gross SJ, Klein W (2002a) Mean-field threshold systems and phase dynamics: an application to earthquake fault systems. *Europhys Lett* 60:481–487
- Tiampo KF, Rundle JB, McGinnis S, Klein W (2002b) Pattern dynamics and forecast methods in seismically active regions. *Pure appl Geophys* 159:2429–2467
- Tsai YB (1986) Seismotectonics of Taiwan. *Tectonophysics* 125:17–37
- Uchida N, Matsuzawa T, Nakajima J, Hasegawa A (2010) Subduction of a wedge-shaped Philippine Sea plate beneath Kanto, central Japan, estimated from converted waves and small repeating earthquakes. *J Geophys Res* 115:B07309
- Wu YM, Chen CC (2007) Seismic reversal pattern for the 1999 Chi-Chi, Taiwan, Mw 7.6 earthquake. *Tectonophysics* 429:125–132
- Wu YM, Zhao L, Chang CH, Hsu YJ (2008a) Focal-mechanism determination in taiwan by genetic algorithm. *Bull Seismol Soc Am* 98:651–661
- Wu YM, Chen CH, Zhao L, Teng TL, Nakamura M (2008b) A comprehensive relocation of earthquakes in Taiwan from 1991 to 2005. *Bull Seismol Soc Am* 98:1471–1481

- Wu YH, Chen CC, Rundle JB (2008c) Precursory seismic activation of the Pintung (Taiwan) offshore doublet earthquakes on 26 December 2006: a pattern informatics analysis. *Terr Atmos Ocean Sci* 19:743–749
- Wu YH, Chen CC, Rundle JB (2008d) Detecting precursory earthquake migration patterns using the pattern informatics method. *Geophys Res Lett* 35:L19304. doi:[10.1029/2008GL035215](https://doi.org/10.1029/2008GL035215)
- Wu YH, Chen CC, Rundle JB (2011) Precursory small earthquake migration patterns. *Terra Nova* 23:369–374
- Wu YH, Chen CC, Rundle JB, Wang JH (2012) Regional dependence of seismic migration patterns. *Terr Atmos Ocean Sci* 23:161–170
- Wyss M, Habermann RE (1988) Precursory seismic quiescence. *Pure Appl Geophys* 126:319–332
- Yoshi T (1979) A detailed cross-section of the deep seismic zone beneath northeastern Honshu, Japan. *Tectonophysics* 55:349–360
- Zoller G, Hainzl S, Kurths J, Zschau J (2002) A systematic test on precursory seismic quiescence in Armenia. *Nat Hazards* 26:245–263

Reproduced with permission of the copyright owner. Further reproduction prohibited without permission.